Emission from dielectric materials at millimeter wavelengths in passive thermal environments

James C. Weatherall

SRA International, Inc., 1201 New Road, Linwood, NJ 08221, USA

ABSTRACT

The brightness of radiation escaping a two-dimensional slab of material under ambient illumination is characterized in terms of its complex dielectric constant. Transmission and reflection coefficients derive from wave optics and the application of Beer's law; the emissivity follows from detailed balancing using Kirchoff's law. The solutions are compared with intensities measured with a commercial millimeter wave imaging system. The results show that millimeter wave imaging of semi-transparent materials can be described by optical physics based on dielectric material properties. In addition, analysis of millimeter wave images of materials could provide information about their dielectric properties.

Keywords: Millimeter waves, terahertz imaging, infrared imaging, security screening, transmission coefficient, reflectivity, dielectric constant

1. INTRODUCTION

Millimeter wave images with ambient illumination are distinguished by differences in the radiation intensity emitted from the surrounding environment and reflected on the target, relative to that emitted by the target itself as thermal emission. In personnel imaging, contrast also depends on how the back illumination by the warm body is transmitted or absorbed by the materials between the person and the camera.

For the purpose of personnel screening, it is important to have knowledge of the electromagnetic properties of materials (embodied in the complex dielectric constant) at millimeter wavelengths, and to understand how these properties govern visibility. The relevant physical measure describing the brightness of an object in millimeter waves is the radiative intensity along the optical path directed towards the observer. In this paper, we present a solution quantifying this measure in terms of the physical properties of the material, its thickness and temperature, and the temperature of the environment in front and back of the material. This solution provides boundary conditions appropriate for personnel imaging. The model is compared with images of dielectric materials obtained with a commercial passive millimeter wave system.

The formulation can be used to carry out image modeling according to the electromagnetic parameters of constituent materials on the target. However, the inverse problem of inferring the electromagnetic properties from millimeter wave images is interesting as well: these properties determine the complex dielectric constant, which is of general importance and is not well documented for materials in millimeter wavelengths.

2. MODEL OF RADIATION ESCAPING AN OBJECT IN A MULTI-PHASE THERMAL ENVIRONMENT

The specific intensity, I, of radiation is the measure of the radiative energy per second per area per solid angle per frequency interval. We employ a two-stream approximation, in which the radiation intensity (which is normally a function of direction) is reduced to a stream I^+ propagating in the direction of the surface normal vector, and I^- in the opposite direction. Fig. 1 shows the model in which the material is a slab between a background at one intensity (temperature), and a foreground at a different intensity (temperature). Note that for temperatures pertaining to personnel imaging environments, the blackbody intensity at frequency ν in the millimeter wave regime, $B(\nu, T)$, can be represented by the Rayleigh-Jeans function, so that the intensity and temperature are related by a multiplicative constant.

E-mail: james_weatherall@sra.com

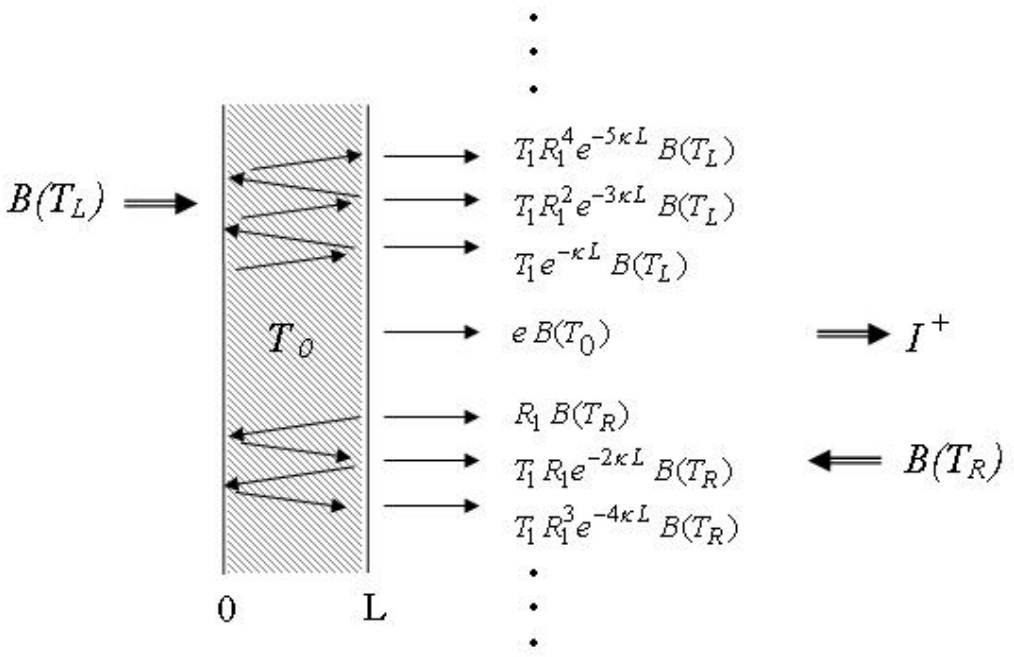

Figure 1. Slab of material at temperature T_0 is illuminated from two sides by external thermal radiation. The radiative intensity is modeled by two streams in the directions normal to the surface. The detected intensity in the stream I^+ is a sum of reflections, transmissions, and emission from the slab.

In the case of a homogeneous medium in this simple geometry, the transmission and reflection amplitudes can be derived using a ray-tracing calculation.[1,2] The single-stream reflectance, defined for normal incidence and a single interface between the medium and air, is given by Fresnel's equations in terms of the medium's index of refraction, n, as $R_1 = |(1-n)/(1+n)|^2$. The single-stream transmittance through the two interfaces of the slab with air is $T_1 = |2n/(1+n)\ 2/(1+n)|^2$. The index of refraction is $n = (\mu\epsilon)^{1/2}$, where ϵ and μ are the susceptibility and permeability in the medium relative to free space. For what follows, we assume μ is unity. This formulation is valid for complex dielectric constant and refractive index.[3] The single-stream transmittance can be written $T_1 = (1-R_1)^2 + 4R_1 sin^2\psi$, where $\psi = arg[(1-n)/(1+n)]$.

For a slab of material illuminated from both sides, the escaping radiation is summed over the multiple internal reflection paths as shown in Fig. 1; the intensity with each transit of the medium is reduced by Beer's law with the intensity absorption coefficient $\kappa = 2n''\omega/c$, where n'' is the imaginary part of the refractive index, $n = n' + in''$. Interference between streams can be ignored when the thickness L of the slab is greater than the temporal coherence length[4] of the radiation. For thermal radiation at 300K, the coherence length is $6\times10^{-4}\ cm$,[5] so the incoherent model is suitable for millimeter waves except for very thin layers. Even for coherent sources, the coherence length $n'c/\Delta\omega$ may still be small due to the bandwidth $\Delta\omega$ of the system, allowing the assumption of phase incoherence.[6] Coherence is also reduced by surface roughness on the order of or larger than the Rayleigh criterion, $\lambda/8$, and by inhomogeneity inside the slab.[1,7] If the phasing among the individual streams does not vary from stochastic effects, the total intensity needs to be computed from summation of electromagnetic fields, rather than addition of intensities as is done here.[1,8] The $\sin\psi$ term in the single-stream transmittance is usually absent in the incoherent model of the reflectance and transmittance.[1,2] This term, which occurs because the electromagnetic waves are inhomogeneous[3] in lossy media, derives from interference between the incident and reflected waves;[9] disregarding it has negligible effect on the net intensity.[1] Thus, the sums over intensities are geometric series that can be simplified into the total intensity reflectance and transmittance:

$$r \;=\; R_1 + \frac{(1-R_1)^2}{1-R_1^2\,\exp(-2\kappa L)}\,R_1\,\exp(-2\kappa L) \qquad (1)$$

$$t = \frac{(1-R_1)^2}{1-R_1^2\,\exp(-2\kappa L)}\,\exp(-\kappa L). \quad (2)$$

Kirchoff's radiation law requires the detailed balancing of absorption and emission in equilibrium, $r+t+e=1$.[2,6] This gives the emission coefficient:

$$e = \frac{(1-R_1)\,[1+R_1\,\exp(-\kappa L)]}{1-R_1^2\,\exp(-2\kappa L)}\,[1-\exp(-\kappa L)]\,. \quad (3)$$

The measurement of intensity made with instrumentation located at the right looking towards the slab corresponds with the stream I^+ (refer to Fig. 1). In terms of the effective reflection, transmission, and emission parameters, the intensity escaping the slab is given by:[6,10,11]

$$I^+ = tB(T_L) + rB(T_R) + eB(T_0). \quad (4)$$

The above solution demonstrates how the millimeter wave appearance of a material changes depending on its absorption, its reflectivity, and its environment. For example, if the temperatures are all the same, there is no contrast between the object and the background, i.e., $I^+ = B(T)$. For optically thin materials, described in the limit $\kappa L << 1$, the contrast between the object and background is principally a function of the material's reflectivity. For absorbing materials, the object's intrinsic thermal emission contributes substantially to the contrast. These properties are summarized in Table 1.

Table 1. Optical Coefficients in Two Thickness Limits

thickness limit	transmittance t	reflectance r	emissivity e
$L << 1/\kappa$	$\frac{1-R_1}{1+R_1}$	$\frac{2R_1}{1+R_1}$	0
$L >> 1/\kappa$	0	R_1	$1-R_1$

2.1 Radiation Escaping an Object with an Opaque Backing Medium

In imaging systems, part of the radiation emanating from an object originates with the human body in close proximity. The human body as a backing medium can be incorporated into the two-stream slab model by modifying the reflectance of the back reflecting surface.

The reflectance presented by a human is frequency dependent.[8,12–14] At 94 GHz, the single-relaxation Debye model of Gandhi[12] gives a value $\epsilon = 6.2 + 9.1i$ for the dielectric constant of skin, which specifies an intensity reflectance at the body/air interface of 34%. In an indoor environment at temperature 20°C, and assuming a core body temperature of 37°C, the millimeter radiometric temperature derived from Eqs. (1)-(4) in the large thickness limit is $20 \times 0.34 + 37(1-0.34) = 31$°C. This is consistent with observations of people at W-band with screening systems.[15]

If the object is in contact with the backing layer, the intensity reflection coefficient $R_2 = |(n-n')/(n+n')|^2$ applies at the interface between the object and the backing layer, where the n' is the complex refractive index of the backing layer. Again utilizing the ray-tracing method, the net power transmittance, reflectance, and emission coefficients are computed for multiple ray paths including the differences at the two interfaces:

$$\tilde{r} = R_1 + \frac{(1-R_1)^2}{1-R_1R_2\,\exp(-2\kappa L)}\,R_2\,\exp(-2\kappa L) \quad (5)$$

$$\tilde{t} = \frac{(1-R_1)(1-R_2)}{1-R_1R_2\,\exp(-2\kappa L)}\,\exp(-\kappa L) \quad (6)$$

$$\tilde{e} = \frac{(1-R_1)\,[1+R_2\,\exp(-\kappa L)]}{1-R_1R_2\,\exp(-2\kappa L)}\,[1-\exp(-\kappa L)] \quad (7)$$

The intensity escaping the slab in contact with the semi-infinite backing is given by Eq. (4), with the temperature T_L equal to the backing medium's core temperature, T', and the reflectance, transmittance, and emissivity given by the backing/slab/air coefficients Eqs. (5) – (7).

2.2 Radiation Escaping an Object with an Air Gap between the Object and an Opaque Backing Medium

If there is an air gap between the object and the backing, the air/slab coefficients Eqs. (1) – (3) can be used with Eq. (4), but T_L is not the core temperature T' of the semi-infinite backing layer. Rather, the effective temperature is computed by solving for T_L in an equation balancing the intensity emitted by and reflected from backing layer with the intensity passing across the gap from the slab: $T_L = 0.34\,(rT_L + eT_0 + tT_R) + (1 - 0.34)T'$. Here, the air/body reflectance is represented by 0.34.

The intensity difference between the two cases can be illustrated with an example. Table 2 shows intensities predicted from Eqs. (1) – (3) and Eqs. (5) – (7) for a range of object temperature and foreground temperature assuming 1 cm of polycarbonate plastic against a human background. (The dielectric parameters for polycarbonate are given in the next section.) Configurations with and without the air gap have differences in intensity amounting to temperature differences of 0.5 – 1.1°C. Although seemingly small, the temperature difference should be compared with the ~ 10°C range between skin and room temperature.

Table 2. Intensity (in Temperature Units) of Polycarbonate Slab

T'	T_0	T_R	$I^+(air\ gap)$	$I^+(no\ gap)$
37	20	20	26.4	25.8
37	37	20	30.2	29.8
37	20	0	18.4	17.3
37	37	0	22.2	21.2

3. COMPARISON OF SLAB MODEL WITH MILLIMETER WAVE IMAGES

The above solution (Eq. 4) is compared with images captured with a commercial millimeter wave imaging camera.*[16] The imaging system is partially enclosed, and provides uniform, temperature-controlled walls both behind and forward of the target. The camera operates in the frequency/bandwidth of 80 GHz – 100 GHz, has a 10 Hz frame rate and a resolution of 25 mm. The images provide intensity data for Makrolon® polycarbonate sheet of different thickness, in varied thermal environments. The polycarbonate sheet slabs have dimensions 10 cm×15 cm×0.635 cm, with different thicknesses obtained by stacking sheets together (with no gaps). A NIST ABC source[17] was used to present a background at an elevated, body-like temperature. The setup is illustrated in the image in Fig. (3), with the polycarbonate target of single sheet thickness outlined in the area on the image. The target is positioned in the foreground between the ABC source and the camera, with the surface normal pointing towards the camera. The eight-bit scaled intensity data is processed in *ImageJ*[18] software by a histogram analysis of 54 pixels overlaying the target, averaged over ten frames; the measured intensity is the intensity mean, and the uncertainty of measurement derives from the standard deviation from the mean.

Fig. (3) shows the measured intensity of polycarbonate slabs in three different illumination environments. In the upper data set (squares), the NIST ABC source at 33.5 °C provides the background illumination. In the middle data set (diamonds), the background illumination is from the back wall. The lower data set (triangles) has the slab backed with a mirror. In scaled units, the intensity of the NIST ABC is observed at $B(T_L) = 218$, the back wall is observed at $B(T_L) = 50.9$, and the foreground intensity, detected using a mirror, is observed at $B(T_R) = 18.5$. An empirical temperature scaling, $B[scaled] = 12.5(T - 16.7)$, was used to convert the temperature of the polycarbonate slab to system units. The polycarbonate material was at room temperature, 25 °C.

*Reference herein to any specific commercial products, processes, equipment, or services does not constitute or imply its endorsement, recommendation, or favoring by the United States Government or the Department of Homeland Security (DHS), or any of its employees or contractors.

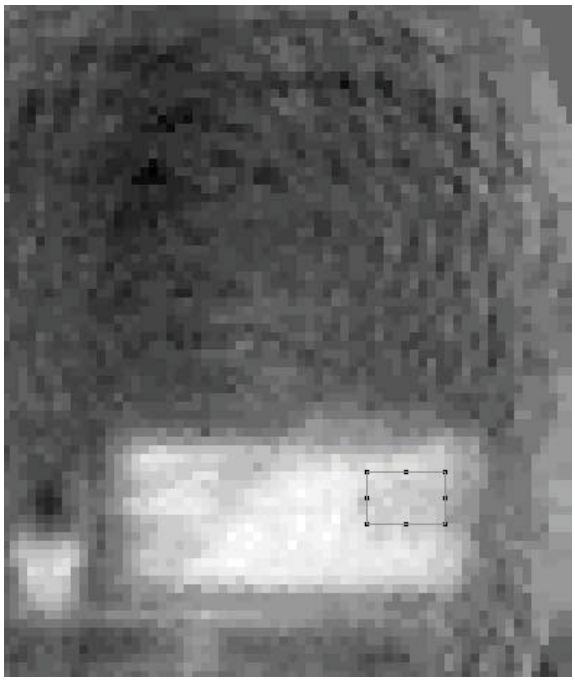

Figure 2. Millimeter wave image of NIST ABC source. The polycarbonate target material is delineated by the outlined box.

The predictions for the model are depicted as lines through the data sets in Fig. (3). The data set backed with the mirror was modeled with $R_2 = 1$ in Eqs. (5) – (7). The value for the complex dielectric of the polycarbonate used for the model was obtained by direct measurement: $\epsilon = 2.77 + 0.015\,i$, with an estimated precision $\Delta\epsilon = \pm 0.02 \pm 0.01\,i$. The measurement was done in free-space over the band 75 GHz – 110 GHz by a transmission/reflection technique, using W-band OML, Inc., source modules connected to an Agilent 8364B PNA network analyzer and 85071E materials measurement software. Although we are not aware of W-band data on polycarbonate in the literature, comparison of the dielectric measurement reported here may be made to data collected in neighboring frequency bands. At 0.3 – 2.4 THz, Ref. 19 reports a real component of the dielectric in the range 2.6 – 2.8, and an imaginary component — affected by THz-band vibrational modes in polymer chains — broadly peaked at 0.080. At 2.484 GHz, Ref. 20 uses $\epsilon = 2.9 + 0.006\,i$ as the dielectric value for polycarbonate. The frequency dependence of the imaginary part illustrates the potential for variability of image intensity across frequency bands. Based on our dielectric measurement, the single-stream reflectance of polycarbonate in W-band is $R_1 = 0.062$, and the intensity absorption coefficient is $\kappa = 0.17\,\mathrm{cm}^{-1}$.

In agreement with the model, the differences in intensity observed in Fig. (3) are due largely to the illumination environment of the objects, particularly for these transparent samples. The trend with increasing thickness (or optical depth κL) is seen to be consistent with the asymptotic behavior predicted by the model, which is that the limiting intensity of a low reflectance material at large optical depth is defined by its brightness in thermal emission (see Table 2). The comparison between model and imaging data indicates that the millimeter wave observation of semi-transparent materials is well-described by the optical physics based on dielectric material properties.

4. INFORMATION IN IMAGES RELATING TO DIELECTRIC CONSTANT

Direct electrical measurement of the dielectric constant of materials can be accomplished with a variety of techniques,[21] but generally involves specialized experimental set ups such as that described in the previous section. Even so, the detection of the imaginary component by transmission/reflection methods is subject to considerable experimental uncertainty.[22] In Sec. 3, it was demonstrated that the intensity of semi-transparent materials imaged in millimeter waves varies with illumination and thickness in a way that is sensitive to the

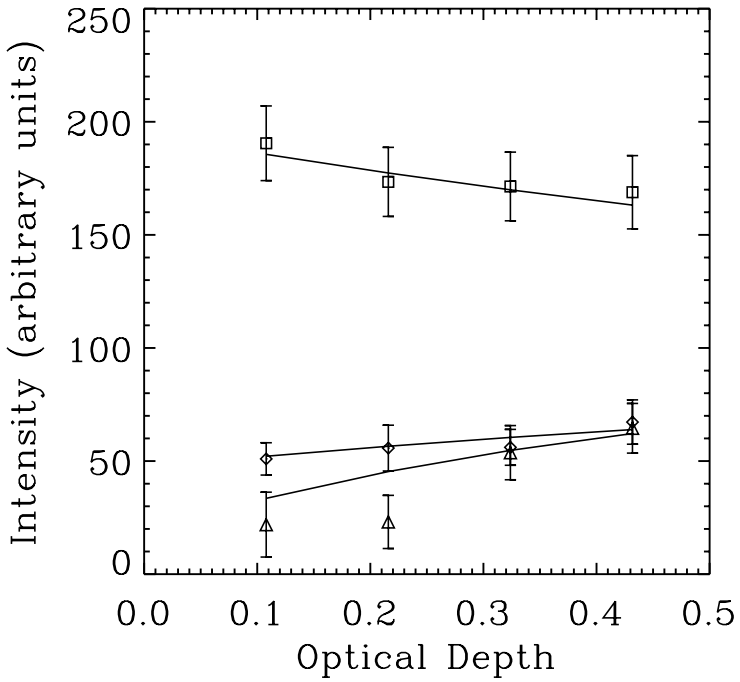

Figure 3. Millimeter wave intensity observed as a function of optical depth, κL, for layered polycarbonate sheet at room temperature in three different environments. The lines are a model fit.

value of the imaginary component of the dielectric constant. This suggests that information obtained by passive millimeter-wave radiometry can be used to infer or put bounds on the complex dielectric constant. For example, models based on different dielectric constants can be compared with image data to see which models best describe the observed intensities.

Comparison of models can be made using a metric consisting of the sum of weighted squared-differences between the model predictions and observations:

$$\chi^2 = \sum_i \frac{1}{\sigma_i^2} \left(I_{obs}(i) - I_{fit}(i) \right)^2 \ , \tag{8}$$

where σ_i is the variance of the intensity of pixels measured over the target image, and the sum is over the images. The best fit is determined by minimizing χ^2 over the free parameters — namely, the real and imaginary components of the dielectric constant. The best fit to the polycarbonate image intensity data obtained in this fashion gives $\epsilon = 2.88 + 0.021\, i$. If the value $\chi^2 = 0.43$ obtained with this solution is used as a chi-square statistic for nine degrees of freedom (twelve data points and two variables), the p-value of the fitting is $p = 0.10$. The dielectric constants that provide a p-value of 0.20 or less suggest a range $\Delta\epsilon = \pm 0.50 \pm 0.005\, i$ (see Fig. 4). The dielectric constant derived by this method overlaps with the value obtained by direct measurement.

The example shows how observations with a passive millimeter wave camera with a multiplicity of slab thicknesses and/or illuminations can be used to solve the "inverse problem" of deriving the dielectric constant.

5. CONCLUSION

Imaging in passive millimeter-wave illumination involves reflection, thermal emission, and transmission through materials. A simple two-stream model for the radiative intensity, as might be applied to materials carried on a person as they are illuminated by thermal emissions from the person and the external environment, has been

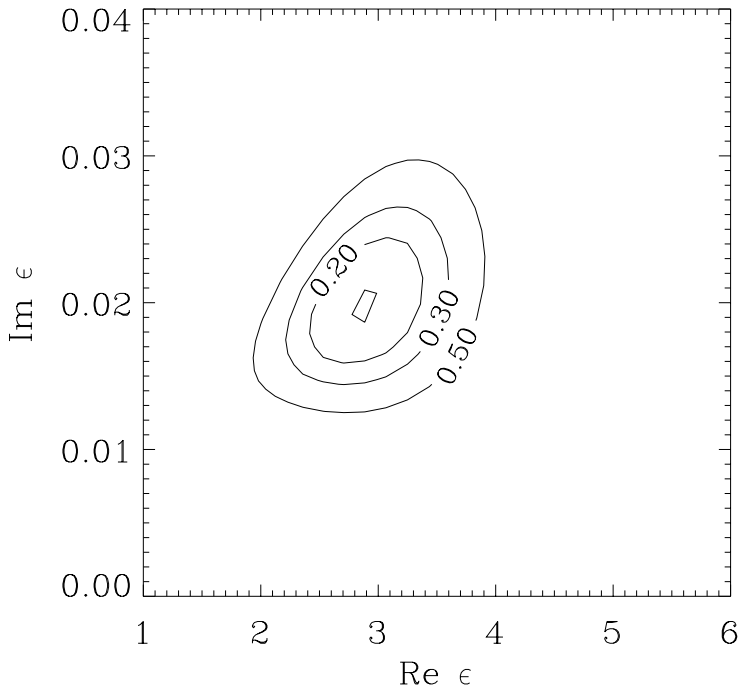

Figure 4. Contours of p-value for dielectric models to polycarbonate slab data.

given here, with emphasis on formulation of the model to include the emission from the materials. Comparing the results to a commercial system shows that the model is suited to the interpretation of millimeter wave signatures of materials.

Millimeter-wave image simulations can be constructed using optical models having multiple radiative streams, by specifying orientation and optical parameters of portions of the target and directions of external sources (see, for example, Refs. 6 and 11). Sophisticated image models might need to include diffuse scattering at the surface and interior of the medium, which will have increasing significance at higher frequencies (such as in the THz region).

It was shown here that a series of images obtained over varied material thicknesses and illuminations provides information about the absorptivity and reflectivity of the material, and this data — obtained with only ambient illumination — can be used to infer dielectric constant.

ACKNOWLEDGMENTS

Work was performed under DHS contract GS-23F-0038L at the Transportation Security Laboratory, Science and Technology Directorate, U.S. Department of Homeland Security, in collaboration with Jeffrey Barber, Loi Tran, and Barry T. Smith. Advice was provided by Charles Dietlein and Douglas Woods. The author is indebted to an anonymous referee for helpful comments.

REFERENCES

[1] Bohren, C. and Huffman, E., [*Absorption and Scattering of Light by Small Particles*], Wiley VCH, Weinheim (2004).

[2] Siegel, R. and Howell, J., [*Thermal Radiation Heat Transfer*], Taylor & Francis, New York, fourth ed. (2002).

[3] Jackson, J. D., [*Classical Electrodynamics*], John Wiley & Sons, New York, third ed. (1998).

[4] Andreasen, J., Cao, H., Taflove, A., Kumar, P., and Cao, C., "Finite-difference time-domain simulation of thermal noise in open cavities," *Phys. Rev. A* **77**, 023810 1–7 (2008).

[5] Mehta, C. L., "Coherence-time and effective bandwidth of blackbody radiation," *Il Nuoveo Cimento* **28**, 401–408 (1963).

[6] Salmon, N. A., "Polarimetric scene simulation in millimeter-wave radiometric imaging," *Radar Sensor Technology VIII and Passive Millimeter-Wave Imaging Technology VII, Proc. SPIE* **5410**, 260 –269 (2004).

[7] Dietlein, C. R., Bjarnason, J. E., Grossman, E. N., and Popović, Z., "Absorption, transmission, and scattering of expanded polystyrene at millimeter -wave and terahertz frequencies," *Passive Millimeter-Wave Imaging Technology XI, Proc. SPIE* **6948**, 69480E (2008).

[8] Alabaster, C. M., "Permittivity of human skin in millimetre wave band," *Electronic Letters* **39**(21), 1521–1522 (2003).

[9] Pincherle, L., "Refraction of plane non-uniform electromagnetic waves between absorbing media," *Physical Review* **72**(3), 232–235 (1947).

[10] Sinclair, G., Anderton, R., and Appleby, R., "Outdoor passive millimetre wave security screening," in [*Security Technology, 2001 IEEE 35th International Carnahan Conference*], 172–179 (Oct 2001).

[11] Grafulla-Gonzales, B., Lebart, K., and Harvey, A. R., "Physical optics modelling of millimetre-wave personnel scanners," *Pattern Recognition Letters* **27**(15), 1852 – 1862 (2006).

[12] Gandhi, O. and Riazi, A., "Absorption of millimeter waves by human beings and its biological implications," *IEEE Transactions on Microwave Theory and Techniques* **34**, 228–235 (Feb 1986).

[13] Pickwell, E., Cole, B. E., Fitzgerald, A. J., Pepper, M., and Wallace, V. P., "In vivo study of human skin using pulsed terahertz radiation," *Physics in Medicine and Biology* **49**(9), 1595–1607 (2004).

[14] Sinclair, G. N., Appleby, R., Coward, P. R., and Price, S., "Passive millimeter-wave imaging in security scanning," *Passive Millimeter-Wave Imaging Technology IV, Proc. SPIE* **4032**, 40–45 (2000).

[15] Martin, C. A., González, C. E. G., Kolinko, V. G., and Lovberg, J. A., "Rapid passive mmw security screening portal," *Passive Millimeter-Wave Imaging Technology XI, Proc. SPIE* **6948**, 69480J (2008).

[16] Millivision Technologies, Inc., South Deerfield, MA, USA, *Portal System 350* (2009). URL: http://millivision.com/portal-350.html.

[17] Dietlein, C., Popović, Z., and Grossman, E. N., "Aqueous blackbody calibration source for millimeter-wave/terahertz metrology," *Appl. Opt.* **47**(30), 5604–5615 (2008).

[18] Rasband, W. S., *ImageJ*. National Institutes of Health, Bethesda, MD, USA (1997-2010). URL: http://rsb.info.nih.gov/ij/.

[19] Kojima, S., Kitahara, H., Nishizawa, S., Yang, Y., and Takeda, M. W., "Terahertz time-domain spectroscopy of low-energy excitations in glasses," *Journal of Molecular Structure* **744-747**, 243–246 (2005).

[20] Han, Q., Hanna, B., and Ohira, T., "A compact espar antenna with planar parasitic elements on a dielectric cylinder," *IEICE Trans Communications* **E88-B**(6), 2284–2290 (2005).

[21] Baker-Jarvis, J., Janezic, M. D., Riddle, B. F., Johnk, R. T., Kabos, P., Holloway, C. L., Geyer, R. G., and Grosvenor, C. A., "Measuring the permittivity and permeability of lossy materials: Solids, liquids, metals, building materials, and negative-index materials," Tech. Rep. 1536, National Institute of Standards and Technology (2005).

[22] Baker-Jarvis, J., Vanzura, E. J., and Kissick, W. A., "Improved technique for determining complex permittivity with the transmission/reflection method," *IEEE Transactions on Microwave Theory and Techniques* **38**(8), 1096–1103 (1990).